Advanced glycation end-products suppress neuropilin-1 expression in podocytes

Tzvetanka Bondeva[1], Christiane Rüster[1], Sybille Franke[1], Elke Hammerschmid[1], Michael Klagsbrun[2], Clemens D. Cohen[3] and Gunter Wolf[1]

[1]Klinik für Innere Medizin III, Friedrich-Schiller-University, Jena, Germany; [2]Department of Surgery and Pathology, Children's Hospital and Harvard Medical School, Boston, Massachusetts, USA and [3]Nephrology Clinic and Institute of Physiology with Center of Integrative Human Physiology, University Hospital and University, Zurich, Switzerland

Advanced glycation end products (AGEs) have been linked to the pathogenesis of diabetic nephropathy. Here we tested the effect of AGE-modified bovine serum albumin (AGE-BSA) on differentiated mouse podocytes in culture. Differential display and real-time PCR analyses showed that in addition to neuropilin-1, the entire signaling receptor complex of neuropilin-2, semaphorin-3A, and plexin-A1, was significantly reduced by AGE-BSA as was neuropilin-1 protein. The effect was specific for podocytes compared to isolated mesangial and tubular epithelial cells. Further, AGE-BSA was not toxic to podocytes. Neutopilin-1 expression was decreased in glomeruli of diabetic *db/db* mice compared to their non-diabetic littermates. Transcripts of both neuropilins were found to be decreased in renal biopsies from patients with diabetic nephropathy compared to transplant donors. Podocyte migration was inhibited by AGE-BSA with similar results found in the absence of AGE-BSA when neuropilin-1 expression was down-regulated by siRNA. In contrast, podocyte migration was stimulated by overexpression of neuropilin-1 even in the presence of AGE-BSA. Our study shows that AGE-BSA inhibited podocyte migration by down-regulating neuropilin-1. The decreased migration could lead to adherence of uncovered areas of the glomerular basement membrane to Bowman's capsule contributing to focal glomerulosclerosis.

Correspondence: *Gunter Wolf, Klinik für Innere Medizin III, Friedrich-Schiller-University, Erlanger-Allee 101, D-07740 Jena, Germany.*
E-mail: Gunter.Wolf@med.uni-jena.de

It has been demonstrated that advanced glycation end products (AGE) formation is increased in diabetes due to chronic hyperglycemia.[1–3] Specific receptors (RAGE) are able to recognize AGEs and initiate various signal transduction pathways resulting in enhanced oxidative stress and transcriptional activation.[3,4] These receptors are localized on podocytes.[4]

Mesangial expansion, a thickening of the glomerular basement membrane, and loss of negatively charged proteoglycans in the glomerular basement membrane, were considered as important structural changes leading to diabetic nephropathy.[5,6] However, recent data suggest that the loss of proteoglycans occurs, if at all, late in the course of diabetic nephropathy.[7] However, significant reduction of the podocyte number per glomerulus and/or podocyte damage occurs early in experimental models of diabetic nephropathy as well as in human diabetic nephropathy.[8–11] Although it has been previously shown that podocytes express RAGE, little is known of potential genetic programs induced by AGEs in these cells. To obtain a better insight into this subject, gene expression was monitored in cultured differentiated mouse podocytes exposed to AGE-modified bovine serum albumin (AGE-BSA) using differential display.

RESULTS

Analysis of AGE-BSA mediated gene expression differences in mouse podocytes

We investigated gene expression in a well-defined differentiated conditionally immortalized mouse podocytes,[12] which were exposed to either 5 mg/ml AGE-BSA or control-BSA (Co-BSA) using differential display analysis. After glycation, AGE-BSA was characterized by a 58-fold higher N^ε-carboxy-methyl-lysine (CML) concentration compared to the Co-BSA (11.6 nmol/mg protein versus 0.2 nmol/mg protein in Co-BSA) and 6-fold higher pentosidine (4.9 pmol/mg protein versus 0.8 pmol/mg protein in Co-BSA) concentrations. Compared with concentrations measured in the serum of patients with type 2 diabetes,[13,14] the used CML concentration was 22.5 times higher but the pentosidine concentration was 5.7 times lower in our cell culture experiments. Co-BSA and AGE-BSA preparations did

Co-BSA

AGE-BSA

Negative control
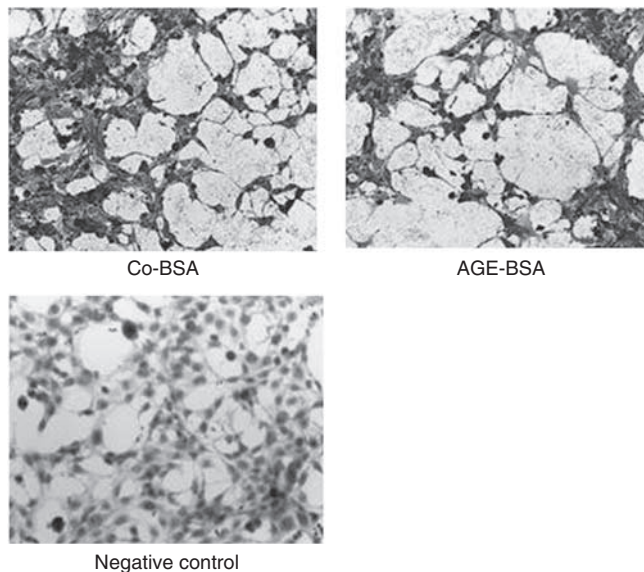
Figure 1 | Immunocytological staining of podocytes for synaptopodin incubated with AGE-BSA 5 mg/ml compared to Co-BSA 5 mg/ml (original magnification 40 ×). Expression of the podocyte differentiation marker synaptopodin did not change after treatment with AGE-BSA. Cells are differentiated and they show signs of arboration. A negative control is shown in which the primary antibody was replaced by normal goat serum.

not contain residual glucose after dialysis (glucose concentration < 0.3 mmol/l). Fluorescence readings were similar to previously reported findings.[15] (5 days: 710 ± 1.4, 15 days: 972 ± 27, 20 days: 1109 ± 19, 50 days: 1173 ± 30 ex 335 nm/em. 420 nm, $n = 6$).

Figure 1 shows that podocytes were differentiated and expressed synaptopodin. AGE-BSA did not influence synaptopodin staining. Gene expression was analyzed in podocytes exposed for 24 h to 5 mg/ml AGE-BSA compared with 5 mg/ml Co-BSA. Partial results from the differential display gel are shown in Figure 2a. We found 188 fragments differentially amplified. From this number 111 PCR bands were upregulated by AGE-BSA compared to the corresponding Co-BSA and 77 fragments were downregulated (data not shown). We have so far identified the sequence for 22 fragments (Table 1).

AGE-BSA inhibits the expression of neuropilin-1 and neuropilin-2 mRNA and protein expression in mouse podocytes

Differential display assays revealed neuropilin 1 (NRP1) as one of the genes, which was downregulated in podocytes by AGE-BSA (Figure 2a). Real-time PCR demonstrated that AGE-BSA reduced mRNA expression of NRP1 by $60 \pm 19\%$ compared to Co-BSA treatment (Figure 2b). As NRPs exist in two isoforms, NRP1 and NRP2, that are found in mouse podocytes,[16,17] we also tested whether AGE-BSA modified the expression of NRP2. mRNA expression of NRP2 in podocytes was also reduced by AGE-BSA compared with Co-BSA (Figures 2b). NRP1 and NRP2 protein expressions were significantly reduced in lysates from the AGE-BSA-treated podocytes compared to the Co-BSA (Figure 2c; NRP1,

Co-BSA: 1.00 ± 0.03, AGE-BSA: $0.65 \pm 0.12^*$; NRP2, Co-BSA: 1.00 ± 0.04, AGE-BSA: $0.60 \pm 0.09^*$ relative expression normalized to vinculin, $n = 10$ for NRP1, $n = 5$ for NRP2, $^*P < 0.01$ versus Co-BSA). NRP1 expression in two syngeneic cell lines, mouse mesangial cells[18] and mouse tubular cells,[19] was present, but its expression was not reduced after AGE-BSA incubation (Figure 2d).

AGE-BSA reduces the expression of genes involved in the neuropilin-1 complex

NRP1 is a binding receptor for semaphorin-3A (Sema 3A) and a coreceptor for the vascular endothelial growth factor $(VEGF)_{165}$.[20] Therefore, we investigated the effect of AGE-BSA on genes involved in the NRP complex. We found that the mRNA expressions of Sema 3A, Sema 3C, and Sema 3F, but not of Sema 3B, is reduced by AGE-BSA (Figure 3a). Moreover, PxA1 mRNA expression was significantly reduced by AGE-BSA, but had no effect on the expression of PxA2, PxA3, and PxB2 (Figure 3b).

AGE-BSA reduced podocyte migration ability through suppression of NRP1

Recently, it was reported that AGE-BSA can inhibit tubulogenesis and migration of kidney epithelial cells.[21,22] Accumulating evidence suggests that NRP1 is involved in the regulation of migration processes in different cell types.[23,24] Therefore, we were interested in assessing the ability of AGE-BSA to affect podocyte migration. 10% fetal calf serum (FCS) induced a significant migration of podocytes (Figure 4a). In comparison with 10% FCS, migration was significantly lower in the presence of Co-BSA (Figure 4a). However, this migration was even further significantly reduced when AGE-BSA was used as stimuli (Figure 4a).

As NRP1 is a receptor for class 3A semaphorins and may act as a coreceptor for $VEGF_{165}$,[20] we tested the ability of mouse $VEGF_{165}$ to affect podocytes migration.[25,26] We first analyzed the expression of VEGF receptor 2 (VEGFR2) in podocytes and found that its expression as detected by western blot was very low (data not shown). Similarly, real-time PCR analysis demonstrated low amounts of VEGFR2 mRNA in podocytes compared to NRP1 expression. AGE-BSA increased and not decreased VEGFR2 expression (NRP1, Co-BSA: 9.7 ± 0.41, AGE-BSA: $10.38 \pm 0.27^*$ ΔC_T; VEGFR2, Co-BSA: $19.32 \pm 0.16^\#$, AGE-BSA: $17.75 \pm 0.20^{\#*}$ ΔC_T, $^*P < 0.05$ versus Co-BSA, $^\#P < 0.001$ versus NRP1 expression, $n = 6$). These results demonstrate that VEGFR2 mRNA expression in podocytes is approximately 1000-fold lower than the mRNA of NRP1 for Co-BSA-treated cells.

Although 1 ng/ml VEGF slightly enhanced migration, this effect was not significant (Figure 4b). 10 ng/ml VEGF alone had no further effect (data not shown). However, the presence of VEGF partially prevented the reduction of migration induced by AGE-BSA (Figure 4b). In addition, Co-BSA compared with 0.1% FCS stimulated migration, indicating a small stimulatory effect albumin (Figure 4b).
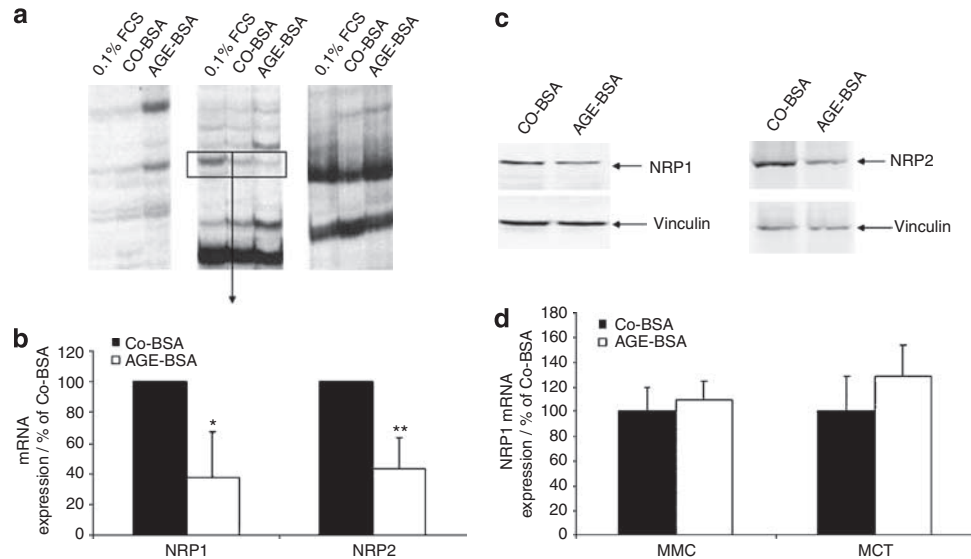
Figure 2 | NRP1 expression. (**a**) Differential display analysis of podocytes treated with 0.1% FCS, 0.1% FCS ± Co-BSA, or 0.1% FCS ± AGE-BSA amplified with three different primer sets demonstrates a number of differentially regulated gene fragments. A small part of the gel is shown as an example demonstrating up- as well as downregulation of various genes. The fragment in the box was excised, subcloned, and sequenced. BLAST analysis revealed that this is the sequence encoding for a NRP1 gene. (**b**) Real-time RT-PCR analysis of NRP1 and NRP2 mRNA expression. AGE-BSA (5 mg/ml for 24 h) significantly reduced mRNA expressions of NRP1 and NRP2 compared to Co-BSA ($n = 6$, *$P < 0.05$, **$P < 0.03$). (**c**) In addition, AGE-BSA also significantly reduced NRP1 and NRP2 protein expressions as determined by Western blots. Equal loading was controlled by anti-vinculin antibody. (**d**) In contrast to podocytes, AGE-BSA failed to downregulate NRP1 mRNA expression in mouse mesangial cells (MMC) and mouse cortical tubular cells (MCT). Real-time RT-PCR, $n = 6$.

Table 1 | Accession numbers of the gene fragments identified by differential display assay

gi|20071927|gb|BC026977.1| Mus musculus N-ethylmaleimide sensitive fusion protein attachment protein gamma, mRNA
gi|111308877|gb|BC120809.1| Mus musculus granzyme N, mRNA
gi|193639|gb|M96930.1| Mus musculus granzyme F gene
gi|50326|emb|X56989.1| Mus musculus CCP4 gene for cytotoxic cell proteinase 4
gi|2275034|emb|AJ000507.1| Mus musculus mRNA for homeodomain protein Meis2d
gi|13810107|emb|AL589699.4| Mouse DNA sequence from clone RP23-92G13 on chromosome 13 Contains the 3′ end of the gene for a novel protein similar to KIAA0386,gi|23304629|emb|AL669844.20| Mouse DNA sequence from clone RP23-395O6 on chromosome 11 Contains the 3′ end of a novel gene
gi|38014372|gb|BC060375.1| Mus musculus WD repeats and SOF domain containing 1, mRNA
gi|41223813|emb|AL928642.5| Mouse DNA sequence from clone RP24-191C1 on chromosome 4 Contains the gene for a novel protein similar to aldolase 1 A isoform Aldo1Mus gi|37805304|gb| BC060129.1| Mus musculus DNA sequence for neuropilin 1, mRNA (cDNA clone MGC:63314)
gi|34808711|gb| BC011073.2| Mus musculus perforin 1 (pore forming protein) (Prf1), mRNA
gi|33859856|gb|AC091783.9| Genomic sequence for Mus musculus, clone RP23-16G10
gi|57544782|gb|AC154829.2| Mus musculus BAC clone RP24-550F10 from chromosome 14
gi|25777708|gb|BC015547.2| Homo sapiens acyl-CoA thioesterase 11 (ACOT11), transcript variant 1, mRNA
gi|1679663|gb|U66473.1| Mus musculus preprogranzyme G gene
gi|77415359|gb|BC106101.1| Mus musculus NSFL1 (p97) cofactor (p47), mRNA
gi|74205898|dbj|AK137088.1| Mus musculus RIKEN full-length enriched library, clone:9430070A02 product:syntaxin binding protein 3gi|24527684|emb|AL928719.6| Mouse DNA sequence from clone RP23-419G21 on chromosome 2
gi|38014372|gb|BC060375.1| Mus musculus WD repeats and SOF domain containing 1, mRNA
gi|54887393|gb|BC085135.1| Mus musculus nucleolar protein 5, mRNA
gi|100818169|gb|BC050875.1| Mus musculus Rho GTPase activating protein 11A, mRNA
gi|89357941|gb|NM030228.2| Mus musculus growth arrest specific 2 like 1 (Gas2l1) protein

The fragments were reamplified, subcloned, and the sequences were subjected to a BLAST search for gene identification.

We next suppressed NRP1 expression by transiently transfecting two different NRP1 siRNA primers or a scramble control siRNA into podocytes. The ability of the two different NRP1 siRNAs to inhibit NRP1 expression was tested with semiquantitative RT-PCR (not shown) as well as by Western blotting (Figure 5a). Downregulation of NRP1 expression led to a significant reduction of the podocyte migration capacity

not only in Co-BSA or AGE-BSA-treated podocytes, but also in podocytes exposed to 10% FCS (Figure 5a). We then performed a contrast experiment by transient overexpression of NRP1. A full-length cDNA of the mouse NRP1 gene was cloned into the pcDNA3 vector. Podocytes were transfected with pcDNA3NRP1 and overexpression was confirmed by Western blots (Figure 5b and c). Transfection with the
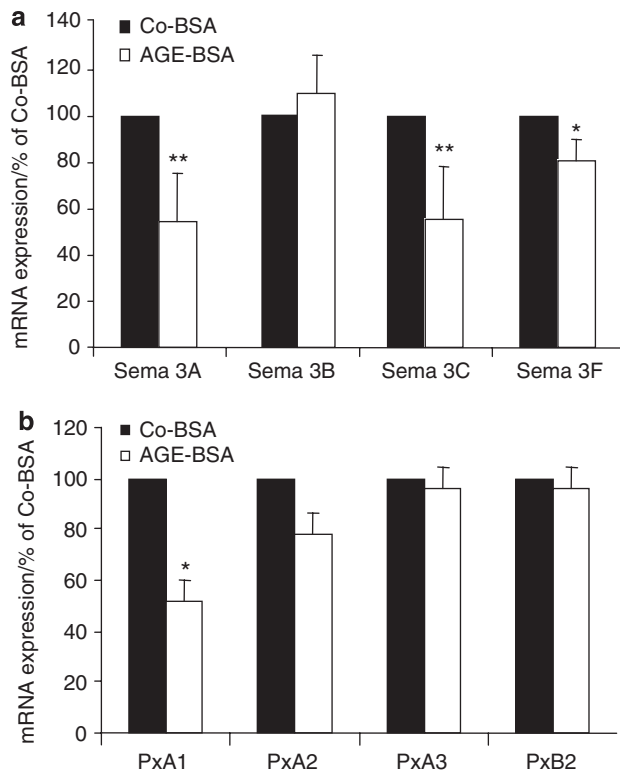
Figure 3 | **AGE-BSA reduced the mRNA expression of other members involved in the NRP1 signaling complex.** (**a**) Expressions of neuropilin ligands semaphorin (Sema) 3A, 3B, 3C, and 3F in podocytes. Except for Sema 3B, mRNA expressions of all other semaphorins were significantly reduced by AGE-BSA incubation (real-time RT-PCR; $n = 6$, *$P < 0.05$, **$P < 0.01$, versus Co-BSA). (**b**) Expressions of neuropilins' signaling-receptors Plexin (Px) A1, A2, A3, and B2 in podocytes. The major coreceptors of NRP1, PxA1, were significantly reduced by AGE-BSA (real-time RT-PCR; $n = 6$, *$P < 0.01$ versus Co-BSA).

Figure 4 | **AGE-BSA suppressed migration of podocytes.** (**a**) Podocyte migration ability was tested in a transwell migration assay system. Addition of AGE-BSA significantly reduced podocyte migration compared to the Co-BSA. 10% FCS was used as a positive control for the migration assay and significantly induced migration. ($n = 16$, *$P < 0.05$ versus Co-BSA, #$P < 0.01$ versus 10% FCS). (**b**) Podocytes migration in transwell assay was also tested using RPMI 1640 medium containing 0.1% FCS (control), 1 ng/ml VEGF$_{165}$, Co-BSA 5 mg/ml, AGE-BSA 5 mg/ml, or 1 ng/ml VEGF$_{164}$ together with Co-BSA or AGE-BSA. VEGF was not able to significantly enhanced migration of podocytes, but attenuated the AGE-BSA-mediated reduction in migration ($n = 16$ *$P < 0.05$ versus Co-BSA). Co-BSA alone significantly stimulated migration compared to 0.1% FCS alone suggesting an effect of albumin ($n = 16$ *$P < 0.05$ versus Co-BSA). N.S. = not significant.
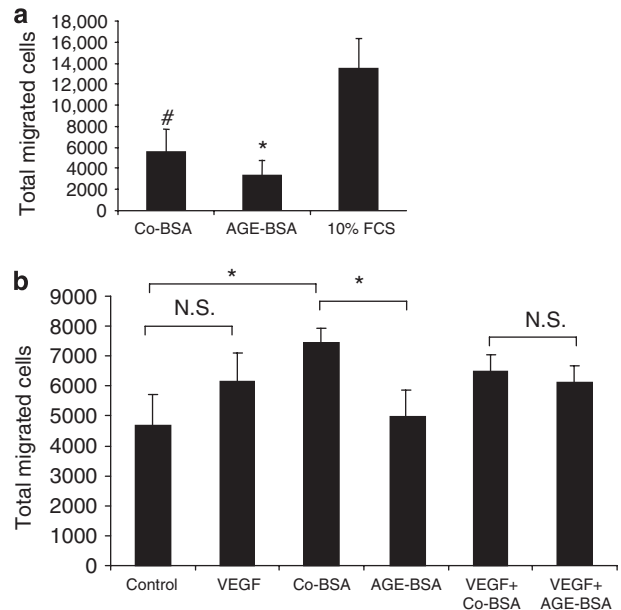
pcDNA3 empty vector did not affect the ability of AGE-BSA to reduce the NRP1 protein expression (Figure 5b). Forced overexpression of NRP1 increased podocyte migration ability even in cells treated with AGE-BSA (Figure 5d).

No cytotoxicity of AGE-BSA for podocytes

To rule out that is the reduced podocytes migration is the presence of AGE-BSA is simply caused by cytotoxicity, we measured lactate dehydrogenase release from damaged cells. Neither Co-BSA nor AGE-BSA was toxic for podocytes (data not shown).

Total suppression of NRP1 with siRNA, but not AGE-BSA, induced apoptosis of podocytes

Recently, it was demonstrated that NRP1 is involved in podocyte survival.[16] Therefore, we addressed the possibility of NRP1 suppression by AGE-BSA to induced podocytes apoptosis. We used CaspAce-FITC-VAD-FMK *in situ* marker as one test for apoptosis.[27] Untransfected podocytes (data no shown) or podocytes transfected with co-siRNA showed no CaspAce-FITC-VAD-FMK staining in the presence of Co-

BSA or AGE-BSA (Figure 6a). However, complete silencing of NRP1 expression with a specific siRNA induced uptake of the CaspAce-FITC-VAD-FMK even in the absence of AGE-BSA (Figure 6b). Suppression of NRP1 mRNA expression by the NRP1 siRNA transfection was controlled by semiquantitative RT-PCR. As shown in Figure 6c, NRP1 siRNA, but not co-siRNA, suppressed very specifically the NRP1, but not NRP2 or glyceraldehyde-3-phosphate dehydrogenase (GAPDH), mRNA expression.

In addition, we also assessed apoptosis by DNA laddering. In accordance with previous studies,[28] AGE-BSA failed to induce fragmentation of genomic DNA isolated from podocytes (Figure 6d). However, complete suppression of NRP1 by siRNA induced DNA fragmentation (Figure 6d).

NRP1 suppression affects podocyte proliferation

We further analyzed the potential role of NRP1 in podocyte proliferation. AGE-BSA significantly reduced bromodeoxyuridine (BrdU) incorporation compared to Co-BSA-treated cells whereas 1 ng/ml VEGF for 24 h stimulated proliferation (Figure 7a). Addition of VEGF to AGE-BSA did not attenuate
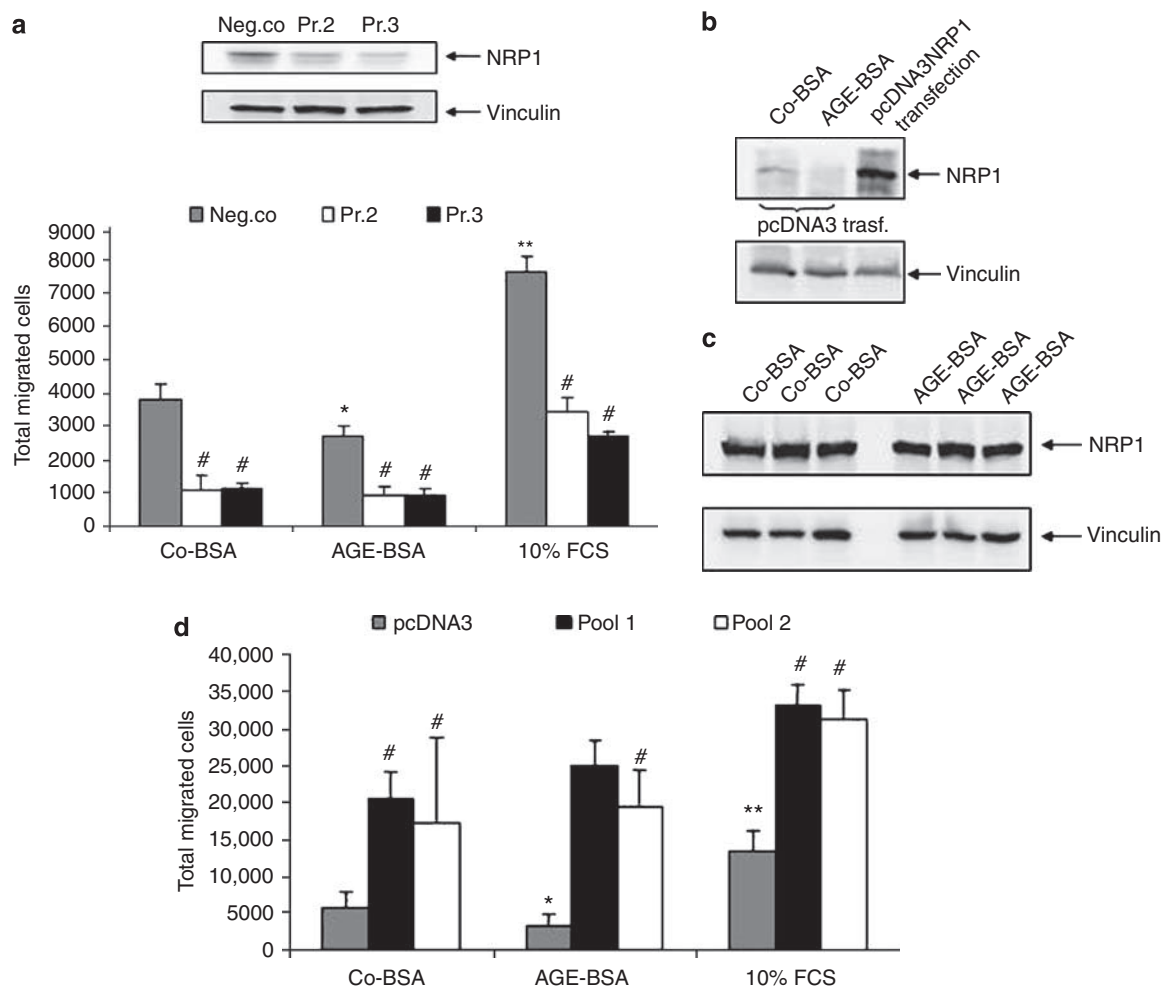
Figure 5 | Effect of neuropilin-1 on podocyte migration. Podocytes migration was analyzed in transwell system. (**a**) Downregulation of NRP1 using siRNA technology reduced podocyte migration. Podocytes were transiently transfected with two different murine NRP1 siRNA primer sets (Pr. 2 and Pr. 3) or a scramble primer as negative control (Neg. co). After transfection, podocytes were allowed to migrate for 24 h. The upper panel of the figure represents a Western blot demonstrating that Pr. 2 and Pr. 3, but not the scrambled primer (Neg. co), reduced NRP1 protein expression. The lower panel shows the results from the migration assay performed after inhibition of NRP1 expression using siRNA. AGE-BSA suppressed and 10% FCS stimulated podocyte migration in the presence of the scrambled primer (Neg. co). However, reduction of NRP1 expression by two different siRNA strongly suppressed podocyte migration even in the absence of AGE-BSA. In these cells, AGE-BSA did not further reduce the migration ability suggesting that no other mechanism besides suppression of NRP1 was operative ($n = 5$, $*P < 0.05$ versus Co-BSA, $**P < 0.01$ versus Co-BSA, $\#P < 0.01$ versus cells transfected with the scrambled control primer (Neg. co). (**b**) Overexpression of NRP1 stimulates migration of podocytes. Transient transfection with the empty pcDNA3 vector did not modulate the AGE-BSA-induced downregulation of NRP1 as shown in this Western blot. (**c**) Forced NRP1 overexpression is not sensitive to AGE-BSA treatment and NRP1 protein levels remain high even in the presence of AGE-BSA. These Western blots represent three different transfection experiments. (**d**) Migration assay. Transfection of podocytes with the empty pcDNA3 vector does not interfere with either the AGE-BSA induced reduction or the stimulation of migration induced by 10% FCS. Pools 1 and 2 refer to two different batches of podocytes being transfected with pcDNA3NRP1. Overexpression of NRP1 significantly stimulated migration of podocytes even in the presence of AGE-BSA and also further increased migration compared with 10% FCS in two different culture batches of podocytes ($n = 16$, $*P < 0.05$ versus Co-BSA, $**P < 0.01$ versus Co-BSA, $\#P < 0.01$ versus pcDNA3 of each condition).

the reduced proliferation and even further reduced proliferation (Figure 7a). Transient transfection of podocytes with NRP1 siRNA, but not with co-siRNA, significantly reduced BrdU incorporation (Figure 7b).

Neuropilin-1 expression is also reduced in diabetic mice
We investigated whether a glomerular suppression of NRP1 occurs in an *in vivo* model of diabetic nephropathy. We used *db/db* mice at 4 months, a widely used model of type 2

diabetes.[29] Blood glucose was significantly enhanced in the *db/db* mice compared to nondiabetic *db/m* mice (*db/db*: 20.84 ± 1.6 mmol/l, *db/m*: 3.98 ± 0.29 mmol/l, $P < 0.01$, $n = 5$). *db/db* mice at 4 months also revealed a significant increase in serum CML and pentosidine compared to nondiabetic *db/m* littermates (CML: *db/m*: 1.15 ± 0.01, *db/db*: $1.86 \pm 0.05^*$ nmol/ml; pentosidine: *db/m*: 6.27 ± 0.45, *db/db*: $12.68 \pm 0.06^*$ pmol/ml; $n = 3$, $*P < 0.05$ versus *db/m*). There was a reduced staining for NRP1 in the glomeruli
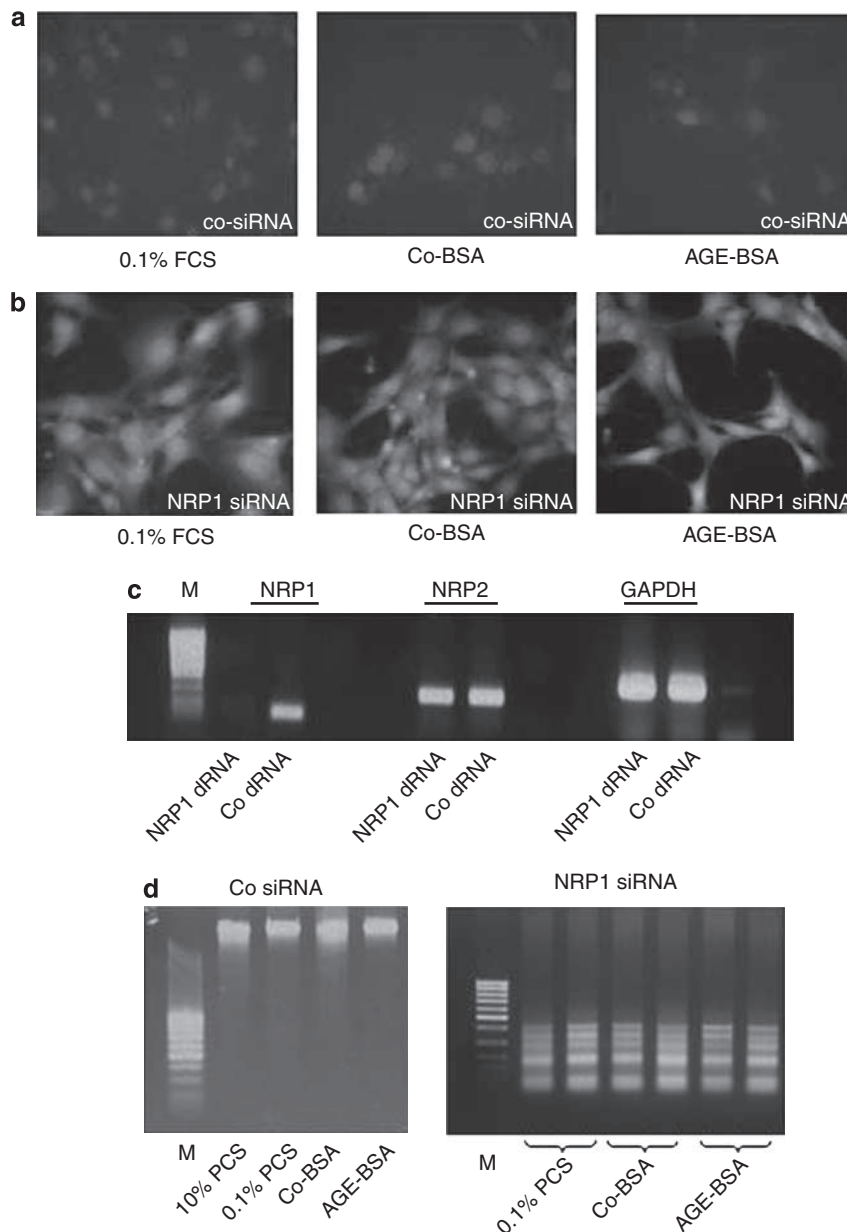
Figure 6 | Apoptosis. (**a**,**b**) Immunohistological detection of caspase activity in podocytes using the cell permeable CaspACE-FITC-VAD-FMK *in sSitu* marker. Podocytes were incubated with RPMI supplemented with 0.1% FCS, Co-BSA, or AGE-BSA for 24 h, followed by 30 min exposure to FITC-labeled pan-caspase inhibitor. (**a**) Detection of caspase activity in podocytes transfected with a nonsilencing co-siRNA. Nuclei were counterstained with DAPI. There are no detectable green apoptotic cells and AGE-BSA did not induce binding of the CaspACE-FITC-VAD-FMK *in situ* marker. (**b**) Detection of caspase activity in podocytes transfected with NRP1 siRNA. In contrast to (**a**), suppression of NRP1 expression by siRNA technology clearly increased the number of green, apoptotic cells. Original magnification × 400. This experiment was independently performed four times with similar results. (**c**) Analyses of podocyte transfection efficiency. Semiquantitative RT-PCRs of mRNA expression of NRP1, NRP2, and GAPDH from podocytes transfected with either NRP1 siRNA or nonsilencing control siRNA (co-siRNA) were performed in parallel to the immunohistological detection of caspase activity. NRP1 siRNA suppresses effectively and specifically NRP1 mRNA but has no effect on NRP2 or GAPDH mRNA expressions and also reduced NRP1 protein expression (see Figure 5a). M = size marker. (**d**) Apoptosis as measured by DNA-laddering. In podocytes transfected with co-siRNA or untransfected (data no shown) AGE-BSA (5 mg/ml for 24 h) failed to degrade genomic DNA. In contrast, inhibition of NRP1 with siRNA induced DNA laddering even in the absence of AGE-BSA. This experiment was independently performed three times with similar results. M = size marker.

of the *db/db* mice compared to the *db/m* animals (Figure 8a and d). To further test the localization of NRP1 expression, kidney sections were double-stained with an antibody against synaptopodin (Figure 8b and e). The double stainings merged (Figure 8c and f) indicating almost an identical expression pattern of NRP1 and synaptopodin. Real-time PCR showed a significant downregulation of NRP1 and Sema 3F mRNA expressions, but not of NRP2 and Sema 3A, in isolated glomeruli from the *db/db* mice compared with the nondiabetic *db/m* littermates (Figure 9).
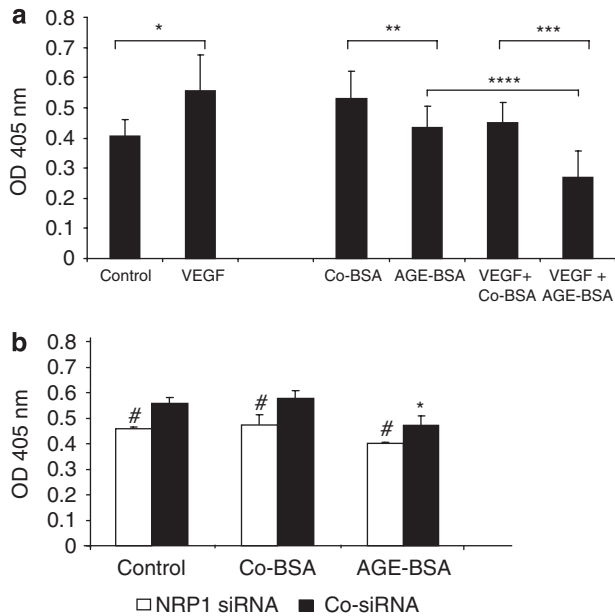
Figure 7 | **Effect of VEGF and AGE-BSA on podocytes BrdU incorporation as a measurement of proliferation.** (**a**) BrdU incorporation was performed using 5×10^3 cells/well in 96-well plates. 1 ng/ml alone VEGF induced cells proliferation, but failed to attenuate the AGE-BSA-mediated reduction in BrdU incorporation. In comparison with AGE-BSA alone, addition of VEGF to AGE-BSA further reduced proliferation ($n = 36$, $*P < 0.05$ versus control, $**P < 0.01$ versus Co-BSA, $***P < 0.05$ versus VEGF plus Co-BSA, $****P < 0.05$ versus AGE-BSA). (**b**) Podocytes were plated at a density 5×10^3 cells/well and were transfected with NRP1 siRNA or control (co) siRNA for 24 h. Podocytes were then incubated with 0.1% FCS (control), Co-BSA or AGE-BSA for 24 h and BrdU incorporation was measured. NRP1 downregulation significantly reduced proliferation in all three conditions. AGE-BSA also significantly reduced BrdU incorporation compared to Co-BSA-treated podocytes. $n = 36$, $^{\#}P < 0.05$ versus co-siRNA of the same treatment groups, $*P < 0.05$ versus Co-BSA.

Expression of NRP1 and NRP2 is reduced in human kidney biopsies from patients with diabetic nephropathy

To further confirm our findings for the human kidney, 15 biopsies of patients with diabetic nephropathy from the European Renal cDNA Bank were investigated.[30] All patients had a serum creatinine > 1.4 mg/dl and clinical details have been previously reported.[31] Normal renal biopsies from living related donors ($n = 8$) served as control. Only microdissected glomeruli were studied. The mRNA expression of NRP1 as well as NRP2 was significantly lower in diabetic nephropathy compared with normal kidneys (NRP1: normal controls: 0.0080 ± 0.0067, diabetic nephropathy: 0.0035 ± 0.0018 NRP1/18S rRNA expression, $P < 0.05$; NRP2: normal controls: 0.013 ± 0.016, diabetic nephropathy: 0.0040 ± 0.0036 NRP2/18S rRNA expression, $P < 0.05$).

DISCUSSION

High concentrations of ambient glucose induced podocyte hypertrophy and stress *in vitro*, suggesting that the podocyte is a likely target of the diabetic milieu.[32] We and others
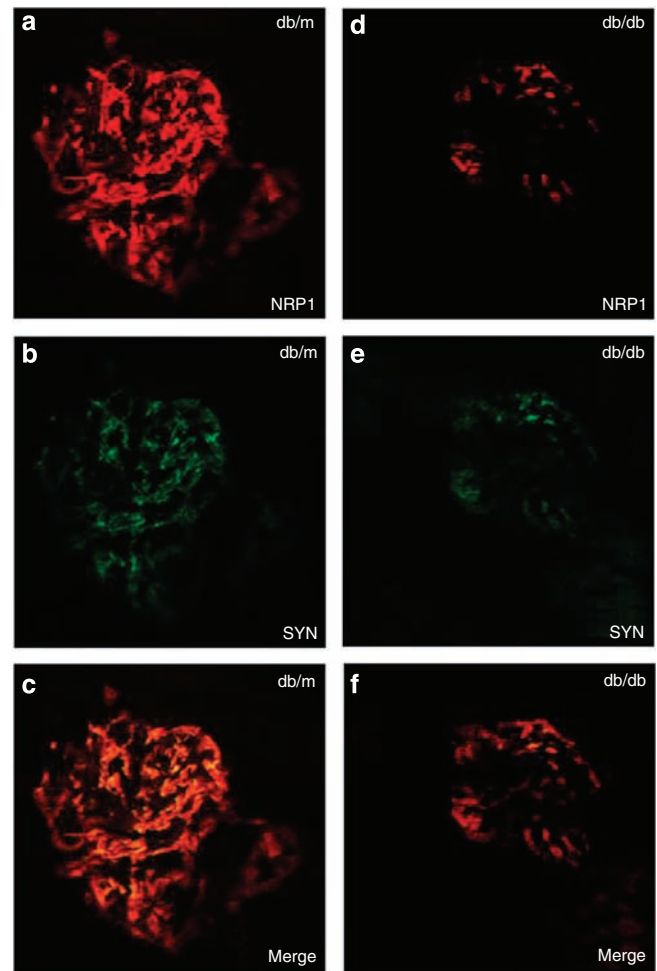
Figure 8 | **Immunohistological detection of NRP1 in kidney glomeruli from diabetic *db/db* and nondiabetic *db/m* mice.** Diabetic (*db/db*) and nondiabetic (*db/m*) mice were perfused and stained for NRP1 (**a** and **d**) or synaptopodin (**b** and **e**). *db/db* mice revealed a decrease in NRP1 staining compared to db/m mice that localized mainly to podocytes as shown in the merged images (**c** and **f**). Original magnification $\times 400$.

reported an increased p27^{Kip1} expression predominantly in podocytes, as the main immunolocalization was detected in podocytes of diabetic rats as well as a high glucose medium induced cell hypertrophy accompanied by the cell-cycle inhibitor p27^{Kip1} upregulation in differentiated podocyte cell lines.[33] We recently described that AGE-BSA inhibited proliferation by arresting podocytes in the G_1-phase of the cell cycle, a process that was mediated by p27^{Kip1}[28] Although transforming growth factor-β may play a role,[34] the full effect of AGEs on podocytes has not yet been clarified and the genetic programs underlying phenotypic changes of podocytes in response to AGEs have been incompletely studied.

Using differential display analysis, we identified NRP1 as one of the genes downregulated by AGE-BSA. AGE-BSA mediated suppression of NRP1 was specific for podocytes and was not caused by unspecific toxic or apoptotic effects of AGE-BSA.
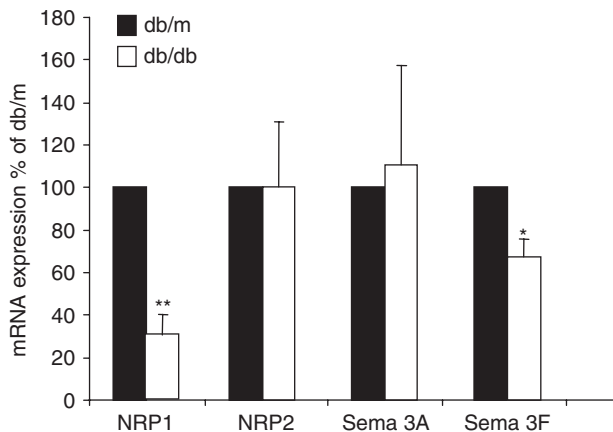
Figure 9 | NRP1 mRNA expression is reduced in kidneys from diabetic *db/db* mice. Total RNAs were prepared from isolated glomeruli, and were reverse transcribed and subjected to real-time PCR. mRNA expressions of NRP1, NRP2, Sema 3A, and Sema 3F were analyzed. mRNA expression is presented as a percent of non = diabetic *db/m* mice. Only NRP1 and Sema 3F, but not NRP2 and Sema 3A, mRNA expressions were reduced in glomeruli harvested from *db/db* mice ($n = 6$ individual mice in each group, $*P < 0.05$, $**P < 0.001$ versus nondiabetic *db/m* mice).

NRP1 expression was also suppressed in podocytes of the diabetic *db/db* mice compared to nondiabetic *db/m* littermates. Although we used double staining of podocytes with the marker synaptopodin, we cannot totally rule out that some mesangial cells also expressed NRP1 in *db/db* mice. However, we believe that the majority of cells exhibiting downregulation of NRP1 expression in *db/db* mice are podocytes and AGE-BSA failed to suppress NRP1 in cultured mouse mesangial cells. Real-time RT-PCR using RNA-prepared isolated glomeruli suggested a decrease in NRP1 transcripts, but not of NRP2. As NRP2 is mainly expressed in lymphatic vessels,[35] one may argue a downregulation of NRP2 is obscured by the presence on lymphatic vessels, but we think that this possibility is not very likely because isolated glomeruli were used for RNA preparation.

In addition, we clearly demonstrated that our findings from cell culture and animal models appear to be true also for the human kidney because patients with diabetic nephropathy revealed significantly less mRNA expression of NRP1 and NRP2 compared with normal kidneys. Certainly, this initial study is limited and it remains to be tested whether these findings are specific for diabetic nephropathy or may also occur in other human glomerulopathies.

NRP1 is a type I cell surface coreceptor that plays important roles in the development of the nervous system and angiogenesis.[36–38] Recently, NRP1 expression in the kidney and particularly in podocytes has been reported.[16–17] During neuronal development, NRP1-mediated signal transduction requires the formation of a functional Sema 3A/NRP1/Plexin A1 complex, which inhibits the axonal guiding signal to the projecting neurons.[24] In endothelial cells, NRP1 enhances the interaction between the heparin binding VEGF$_{164/165}$ with its VEGFR2 and modulates VEGF-depen-

dent angiogenesis.[39,40] We found that AGE-BSA specifically affect the expression of the NRP1 and NRP2 receptor complexes and their ligands Sema 3A and Sema 3F. Stimulated by recent studies by Gallichio *et al.*[22] showing that AGEs are capable of regulating tubulogenesis and migration of kidney epithelial cells, as well as a potential involvement of NRP1 in cell movement in other cell types, we performed migration studies in podocytes treated with AGE-BSA or Co-BSA. AGE-BSA inhibited the migration of podocytes. We clearly showed through various approaches that this effect was mediated by a downregulation of NRP1. Our study using anti-NRP1 siRNA technology as well as forced overexpression of NRP1 demonstrated that the decrease in podocyte migration induced by AGE-BSA is not an unspecific toxic effect, but depended on the suppression of one gene, namely NRP1. We also addressed VEGF dependent migration in podocytes. Under our experimental conditions VEGF did only marginally, but not significantly, stimulated migration. However, VEGF attenuated the AGE-BSA reduced podocyte migration. We are convinced that the AGE-BSA-induced downregulation of NRP1 leading to a decrease in podocyte migration is detrimental for podocyte structure and function, as the inability of podocytes to migrate leads to 'nude' areas of the glomerular basement membrane which subsequently adheres to Bowman's capsule initiating focal glomerulosclerosis.[11,41]

In accordance with previous studies from our group, AGE-BSA alone did not induce apoptosis of podocytes.[28] However, total silencing of NRP1 with siRNA technology readily induced apoptosis of podocytes as measured by two different assays. This finding suggests that the AGE-BSA-mediated downregulation of NRP1 by approximately 60% is not sufficient to induce apoptosis. As a speculation, if additional factors, induced by the diabetic environment, lead to further NRP1 reduction, apoptosis may occur and contribute to podocytes loss in diabetic nephropathy.

Guan *et al.*[16] have recently also described the presence of the semaphorin system in podocytes. Interestingly, they found that podocytes exposed to recombinant exogenous Sema 3A induced downregulation of podocin and decreased its interaction with CD2-associated proteins and nephrin.[42] Although it is difficult to compare endogenous to exogenous concentrations of Sema 3A, a downregulation of Sema 3a by AGE-BSA as found in our study can be seen as an ultimately unsuccessful attempt to maintain the homeostasis of slit-diaphragm proteins and to counteract apoptosis. On the other hand, it has been found that the VEGF-A system is necessary for upregulation of podocin and its interaction with CD2AP.[42] Moreover, VEGF-A is also required for mesangial cell survival and differentiation.[25,26] As NRP1 and NRP2 are coreceptors for VEGF, a downregulation of NRP1 and NRP2 may attenuate VEGF signaling, particularly in light of the fact that not all studies have found expression of VEGFR1 and VEGFR2 receptors on podocytes. Indeed, a recent study has shown that glycated albumin interferes with VEGF signaling.[43] We were able to confirm that VEGFR2 is

expressed in cultured podocytes but its expression is very low compared to the NRP1 expression. We believe that our data also demonstrate that proliferation and migration of podocytes are complexly associated. VEGF plays a role in podocytes survival but fails to attenuate the AGE-BSA-induced reduction in proliferation, presumably because AGE-BSA arrests the cells in the G_1-phase via a mechanism involving p27[Kip1] induction that cannot be overcome even in the presence of VEGF.[28] Tapia *et al.*[44] recently described that exogenous Sema 3A decreased VEGFR2 receptor signaling and causes acute proteinuria that was antagonized by administration of VEGF. These very interesting findings indicate that a delicate balance of Sema 3A and VEGF is important for glomerular filtration barrier homeostasis. We suggest that this balance can be also disturbed by suppression of NRP1, and the complex interactions among NRP1, Sema 3A, and VEGF certainly require further studies.

In summary, our data show that AGE-BSA suppresses the NRP1 and NRP2 receptor systems and that this leads to a decrease in podocyte migration. These pathophysiological changes may have profound implications for podocyte pathology through various mechanisms in diabetic nephropathy.

MATERIALS AND METHODS
Preparation of AGE-BSA
BSA (Fraction V, fatty acid-poor, endotoxin-free; Calbiochem, La Jolla, CA, USA) was incubated under sterile conditions at 37 °C for 50 days in phosphate-buffered saline (PBS) with and without the addition of glucose 90 mg/ml and filtrated (Millipore Labscale TFF System, Billerica, MA, USA), extensively dialyzed against PBS, glucose concentration measured (hexokinase method), and lyophilized. Samples (2 mg/ml AGE-BSA) from different time points (5–50 days) were measured at an emission of 420 nm after excitation at 355 nm using a fluorescence reader FLUOstar OPTIMA (BMG Labtech, Offenburg, Germany). CML was measured by an ELISA (Roche Diagnostics, Mannheim, Germany) and pentosidine was determined by HPLC as previously described.[13,14]

Cells and cell culture
Conditionally immortalized mouse podocytes were grown in RPMI 1640 medium with stable glutamine (PromoCell GmbH, Heidelberg, Germany) supplemented with 10% heat-inactivated FCS in the presence of recombinant mouse γ-interferon (10 U/ml) for 3 weeks at 33 °C and 5% CO_2.[12,45] Removal of the γ-interferon and temperature switch to 37 °C induced podocyte differentiation. Differentiated podocytes were tested positive for synaptopodin by immunohistochemistry. These differentiated podocytes, named later only podocytes, were used for our experiments. Mouse mesangial cells[18] and mouse epithelial tubular cells,[19] were grown in Dulbecco's modified Eagle's medium with stable glutamine containing 10% heat-inactivated FCS. Mouse VEGF$_{165}$ was ordered from Sigma (Taufkirchen, Germany) and used in concentration 1 and 10 ng/ml.

Differential display
Mouse podocytes were incubated with AGE-BSA (5 mg/m) or the same concentration Co-BSA for 24 h in the presence of 0.1% FCS.

Total RNA was isolated with the RNA easy kit (Qiagen, Hilden, Germany) from both groups. Differential display PCR was performed with RNAimage GenHunter (WAK-Chemie Medical, Steinbach, Germany) and was theoretically capable of amplifying gene sequences by 24 combinations of three 1-base anchored oligo-dT primers (H-T$_{11}$A, C, G) and eight random 13-mer primers (AP1-8). Briefly, 0.2 µg DNA-free total RNA was reverse transcribed by oligo-dT primer to produce the first-strand cDNA. One-tenth of the first-strand reaction mixture was used as a template for PCR, which was performed according to the following conditions: 94 °C for 3 min; 40 cycles at 94 °C for 30 s, 40 °C for 2 min, and 72 °C for 1 min; and 72 °C for 5 min. α-[^{33}P]dATP was incorporated into the PCR products, which were displayed on a 6% denatured sequencing gel and visualized by autoradiography. The candidate differentially expressed fragments were cloned into the vector pCRII-TOPO (Invitrogen, Karlsruhe, Germany) and sequenced. The sequences were subjected to BLAST search for further analysis and identification.

Reverse-transcription and semiquantitative polymerase chain reaction
Total RNA was isolated from 1×10^6 podocytes cultured for 24 h in RPMI 1640 medium containing 0.1% heat inactivated FCS, or RPMI 1640 medium supplemented with 0.1% FCS plus Co-BSA (5 mg/ml) or with 0.1% FCS plus AGE-BSA (5 mg/ml). cDNA was generated from 1–2 µg total RNA using M-MLV Reverse Transcriptase kit (Invitrogen). From the resulting cDNA 2 µl were subjected to PCR amplification by the use of gene specific primers (Table 2). PCR amplifications were performed as follows: 95 °C for 5 min, 95 °C for 45 s, annealing temperature as indicated in Table 2 for 45 s, 72 °C for 45 s, repeated 30–35 cycles, and a last elongation step at 72 °C for 5 min. The cDNA for mouse GAPDH was amplified as a control.

Table 2 | Sequence and annealing temperature of the primers used for sem-quantitative and real-time PCR analyses of the corresponding genes

Primer	Sequence	Annealing temperature (°C)
NRP1	Fw 5′-GAAGGCAACAACAACTATGA-3′ Rev 5′-ATGCTCCCAGTGGCAGAATG-3′	58 °C
NRP2	Fw 5′-AAGTGGGGGAAGGAGACTGT-3′ Rev 5′-GTCCACCTCCCATCAGAGAA-3′	58 °C
Sema 3A	Fw 5′-GTTGTAGACCGGGTGGATGC-3′ Rev 5′-TCGGAGCAGTGAGTCAGTGG-3′	58 °C
Sema 3B	Fw 5′-GAGGACTCTGCCGCTATCAC-3′ Rev 5′-CTCCACACCCAACACCTTCT-3′	56 °C
Sema 3F	Fw 5′-AGGTGGATGCAGCTGATGG-3′ Rev 5′-GGAATTGAAACCACGGCACT-3′	60 °C
Sema 3C	Fw 5′-GCAAAATGGCTGGCAAAGATCC-3′ Rev 5′-CCCATGAAATCTATATACATTCC-3′	60 °C
PxA1-3	Fw 5′-CCTCGAGAACAAGAACCACCCCAA-3′	
PxA1	Rev 5′-CCCTTCACCGGCACCTCAGGTGCATT-3′	58 °C
PxA2	Rev 5′-AACACCTTCACTGGGATCTCTGGACTGTTC-3′	60 °C
PxA3	Rev 5′-CTTCACTGGGACCTGGGCGCTGCC-3′	56 °C
PxB2	Fw 5′-GATGGAGGACCAGACGAATGA-3′ Rev 5′-CAGACCTGCGCAGCATTAGC-3′	58 °C
VEGFR2	Fw 5′-GCTTTCGGTAGTGGGGATGAA-3′ Rev 5′-TTGGTGAGGATGACCGTGTA-3′	58 °C
GAPDH	Fw 5′-TGTCAGCAATGCATCCTGCA-3′ Rev 5′ GATGTCATCATACTTGGCAGGTT-3′	60 °C
β-Actin	Fw 5′-GATGATGCAGATAATGTTTGAAAC-3′ Rev 5′-GAGCAATGATCTTAATCTTCATTGTG-3′	60 °C

Cloning of the mouse NRP1 gene

Murine NRP1 gene was amplified from cDNA synthesized from the total RNA isolated from podocytes grown in normal growth medium. The gene was amplified in two fragments using the following primers: mNP1F/NRP1R and NRP1F/mNP1R from Table 2. The amplified fragments were cloned into the PCRII-TOPO vector and further cloned into pcDNA3. The NRP1 gene was completely sequenced by automatic sequencing.

Real-time RT-PCR

Real-time PCR for mRNA determination was done in a final volume of 20 μl containing 1 μl of cDNA, 0.5 μM of each sense and antisense primers, and 4 μl master mix of Lightcycler FastStart DNA Master ^{PLUS} SYBR Green I kit from Roche Applied Science (Mannheim, Germany). Real-time PCR reactions were performed on a LightCycler instrument (Eppendorf AG, Hamburg, Germany) according to the standard manufacturer protocols. The expression of the gene of interest and GAPDH mRNA was analyzed with monoplex analysis in which the target gene and the housekeeping gene (GAPDH) were simultaneously determined in two different reactions, both detected under the same dye (SYBR Green) in a 96-well plate. The measurements for the target gene and GAPDH mRNAs were set up as subassays. The threshold cycle (C_T) represents the PCR cycle at which an increase of the reporter fluorescence above the baseline is first detected. The relative quantification analysis module is used to compare expression levels of the target gene among differently treated samples. The expression levels are calculated using the $\Delta\Delta C_T$ method.[46] A prerequisite to yield valid relative expression values is that the efficiency is comparable and close to 1 in the PCR systems of both the target and the housekeeping gene. The expression levels R are calculated as follow: $R = 2^{-\Delta\Delta CT}$ (where $R = 2^{(\Delta CT \; treated - \Delta CT \; control)}$).

Downregulation of NRP1 with Mouse NRP1 siRNA

Podocytes were plated in six-well plates at density 2×10^5 to 3×10^5 cells/well in 1 ml RPMI medium, containing 8% FCS. The next day the cells were transfected using HiPerfect transfection reagent (Qiagen) with two different mouse NP1 siRNA primers Mm_Nrp1_2 HP siRNA and Mm_Nrp1_3 HP siRNA and a control primer (all from Qiagen) following the manufacturer instructions. Concentrations of 10 nM (75 ng) and 20 nM (150 ng) from the corresponding mouse NRP-1 siRNA primers, or the same concentrations of the scramble primer, were used for transfection. The cells were incubated with the transfection complexes under normal growing conditions RPMI medium, 8% FCS. Twenty-four hours after transfection the suppression of NRP-1 mRNA was confirmed by RT–PCR using the Mm_Nrp1_1_SG QuantiTect Primer Assay (Qiagen) and cells were then further subjected to different assays and analysis as needed. All experiments were performed in triplicates.

Western blot analysis

Podocytes were incubated as described, washed with PBS, and lysed in buffer containing 50 mM Tris-HCL, pH 7.4; 100 mM NaCl; 2.5 mM MgCl$_2$; 1% Triton X-100, supplemented with 1 mM PMSF, 1 mM Na$_3$VO$_4$, and cocktails of protease inhibitors (Boehringer, Mannheim, Germany). SDS–polyacrylamide gel electrophoresis and Western blotting were performed as described elsewhere.[35] To assess the protein expression of NRP-1 and NRP-1 the membrane was further incubated for an additional 1 h with polyclonal antibodies against mouse NRP-1 as well as NRP-2 (Abcam,

Cambridge, UK) in dilution 1:500 in 5% BSA-TBST, washed several times with TBST, and incubated for 1 h with a horseradish peroxidase conjugated goat anti-rabbit secondary antibody (1:5000; KPL, Gaithersburg, MD, USA). The vinculin monoclonal antibody was from Sigma. After intensive washing the proteins were visualized with ECL detection reagent (Roth, Karlsruhe, Germany).

Cell migration assay

Podocytes were adjusted to a concentration of 0.5×10^6 to 1×10^6 cells/ml in serum-free medium and subjected to a transwell migration assay using a Boyden chamber. Cell suspension (300 μl) was plated on 8 μm membrane pore size cell inserts (Nunc, Langensbold, Germany) in the upper chamber. 500 μl of the medium containing the reagent that needed to be tested was added to the lower chamber and the cells were incubated for 24 h. All treatments were performed in triplicate. After the incubation time, the inserts were placed in new wells containing 200 μl of the prewarmed accutase (Innovative Cell Technologies, San Diego, CA, USA) and incubated for 30 min at 37 °C to remove the cells from the lower side of the insert by gently shaking the insert back and forth several times during the incubation. The total cell number for each separate well was counted in a Coulter counter.

LDH release assay

Potential cytotoxicity induced by Co-BSA or AGE-BSA treatment was evaluated by the quantification of the lactate dehydrogenase release from damaged cells using the lactate dehydrogenase cytotoxicity assay kit (BioVision Research Products, Mountain View, CA, USA).

Proliferation assay

BrdU incorporation (Roche Diagnostics) was used as a parameter for DNA synthesis. Podocytes were grown in a 96-microtiter plate with 5000 cells/well. After that media was supplemented with Co-BSA or AGE-BSA (5 mg/ml), or VEGF$_{165}$ (1 or 10 ng/ml) and incubated for another 24 h. BrdU labeling reagent was added for 4 h. Fixation of cells, and detection of BrdU was performed according to the manufacturer's protocol. Each measurement was performed with $n = 12$ per treatment group. The tests were independently repeated three times.

Analysis of apoptosis

Podocytes were plated in chambers slides and were transfected with 20 nmol of each NRP1 siRNA, or nonsilencing control siRNA or were left untransfected. Transfection mixtures were exchanged with RPMI medium containing 0.1% FCS, Co-BSA, or AGE-BSA and the cells were incubated for 24 h. CaspACE-FITC-VAD-FMK *in situ* marker (Promega, Madison, WI, USA), a cell permeable fluorescent analogue of the pan caspase inhibitor Z-VAD-FMK (carbobenzoxy-valyl-alanyl-aspartyl-[*O*-methyl]-fluoromethylketone) was added at a final concentration 5 μM for 30 min at 37 °C The cells were washed twice with PBS, fixed with 10% formalin in PBS buffer for 30 min at room temperature. Slides were washed three 3 times with PBS, mounting medium and cover slips were added, and the cells were analyzed under a fluorescence microscope Axioplan (Zeiss, Germany). In addition, apoptosis was also assessed by DNA laddering. Podocytes were plated at density 4×10^5 cells/well into six-well plates and incubated as appropriate. Cells were washed once with PBS and genomic DNA was isolated using DNAeasy Tissue kit (Qiagen) according to the manufacturer's instructions. Finally, the

genomic DNA was eluted with 100 µl buffer. After that the quality of the purified genomic DNA was analyzed on 0.8% agarose gel.

Animal experiments

Animal experiments were approved by the local Animal Care Committee of the University of Jena and done in accordance with the German Animal Protection Law. Male *db/db* (B6.Cg-*m* + / + *Lepr*^*db*^/J; Jackson Laboratory, Bar Harbor, ME, USA) mice at 4 months and their age-matched nondiabetic *db/m* littermates were used. Kidneys were perfusion fixed before harvesting. In addition, kidneys were also harvested without perfusion and glomeruli were isolated by differential sieving techniques as described.[18]

Immunocytology and immunohistochemistry

For cultured podocytes, cells were grown on glass cover slips at a density of 4×10^5 and were incubated with Co-BSA or AGE-BSA for an additional 24 h. Cells were fixed with 4% paraformaldehyde, and synaptopodin was detected with a rabbit antibody (Sigma) and indirect immunocytochemistry. Immunohistochemistry was performed as described elsewhere in detail.[47] The primary NRP1 rabbit antibody (Calbiochem) or synaptopodin (polyclonal goat, NE-14; Santa Cruz Biotechnology, Santa Cruz, CA, USA) antibodies were used in dilution 1:250 and incubated overnight at 4 °C, and the secondary antibody rabbit anti-goat-FITC conjugated (Delta Biolabs, Gilroy, CA, USA) or donkey anti-rabbit-Cy3 conjugated (Jackson ImmunoResearch Lab, West Grove, PA, USA), were used in dilution 1:1000 for 3 h. Negative controls were performed using nonimmune sera from the appropriate species to replace the primary antibody. Cells or the kidney sections were washed several times with PBS and embedded in Kaiser's gelatin. For a double staining on kidney slides first the sections were incubated with the primary NRP1 antibody, then with the secondary antibody, followed with new blocking and staining with anti-synaptopodin antibody. Immunohistochemistry was performed on five different animals from each group.

Human kidney biopsies

Human kidney biopsies were obtained from patients after informed consent and with approval of local ethic committees as part of the European Renal cDNA Bank. Material was submerged in an RNAse inhibitor (RNAlater; Ambion, Austin, TX, USA) and microdissected under standardized conditions at the core facility as previously described.[30] Pretransplant biopsies from 8 living donors served as controls. A total of 15 biopsies from patients with diabetic nephropathy were studied. The clinical details of these patients have been previously described.[31] NRP1 and NRP2 expression was studied in microdissected glomeruli at the core facility by established methods as previously described in detail.[30] Predeveloped TaqMan reagents were used for human NRP1, NRP2, and 18S rRNA on a 7500 Fast Real-Time PCR System (all Applied Biosystems, Darmstadt, Germany). The mRNA expression was analyzed by standard curve quantification. Normalization was performed for the expression of the 18S rRNA housekeeping gene.[30,31]

Statistical analysis

All data are reported as means ± standard deviation (s.d.). Statistical analysis was performed using the statistical package SPSS for Windows version 11.0 (SPSS Inc., Chicago, IL, USA). Results were analyzed with the Kruskal–Wallis test followed by Mann–Whitney *U*-test. Differences were considered significant when $P < 0.05$.

REFERENCES

1. Brownlee M. Glycation and diabetic complications. *Diabetes* 1994; **43**: 836–841.
2. Bohlender JM, Franke S, Stein G *et al*. Advanced glycation end products and the kidney. *Am J Physiol Renal Physiol* 2005; **289**: F645–F659.
3. Thomas MC, Forbes JM, Cooper ME. Advanced glycation end products and diabetic nephropathy. *Am J Ther* 2005; **12**: 562–572.
4. Wendt TM, Tanji N, Guo J *et al*. RAGE drives the development of glomerulosclerosis and implicates podocyte activation in the pathogenesis of diabetic nephropathy. *Am J Pathol* 2003; **162**: 1123–1137.
5. Wolf G, Ziyadeh FN. Cellular and molecular mechanisms of proteinuria in diabetic nephropathy. *Nephron Physiol* 2007; **106**: p26–p31.
6. Dalla Vestra M, Saller A, Mauer M *et al*. Role of mesangial expansion in the pathogenesis of diabetic nephropathy. *J Nephrol* 2001; **14**(Suppl 4): S51–S57.
7. Van den Born J, Pisa B, Bakker MA *et al*. No change in glomerular heparan sulfate structure in early human and experimental diabetic nephropathy. *J Biol Chem* 2006; **281**: 29603–29613.
8. Wolf G, Chen S, Ziyadeh FN. From the periphery of the glomerular capillary wall toward the center of disease: podocyte injury comes of age in diabetic nephropathy. *Diabetes* 2005; **54**: 1626–1634.
9. Nosadini R, Velussi M, Brocco E *et al*. Course of renal function in type 2 diabetic patients with abnormalities of albumin excretion rate. *Diabetes* 2000; **49**: 476–484.
10. Hoshi S, Shu Y, Yoshida F *et al*. Podocyte injury promotes progressive nephropathy in Zucker diabetic fatty rats. *Lab Invest* 2002; **82**: 25–35.
11. Kriz W, Gretz N, Lemely KV. Progression of glomerular diseases: is the podocyte the culprit? *Kidney Int* 1998; **54**: 687–697.
12. Mundel P, Reiser J, Zuniga Mejia Borja A *et al*. Rearrangements of the cytoskeleton and cell contacts induce process formation during differentiation of conditionally immortalized mouse podocyte cell lines. *Exp Cell Res* 1997; **236**: 248–258.
13. Busch M, Franke S, Wolf G *et al*. The advanced glycation end product N^ε^-carboxymethyllysine is not a predictor of cardiovascular events and renal outcomes in patients with type 2 diabetic kidney disease and hypertension. *Am J Kidney Dis* 2006; **48**: 571–579.
14. Busch M, Franke S, Wolf G *et al*. Serum levels of the advanced glycation end products N^ε^-carboxymethyllysine and pentosidine are not influenced by treatment with the angiotensin receptor blocker II type 1 blocker irbesartan in patients with type 2 diabetic nephropathy and hypertension. *Nephron Clin Pract* 2008; **108**: c291–c297.
15. Valencia JV, Weldon SC, Quinn D *et al*. Advanced glycation end product ligands for the receptor for advanced glycation end products: biochemical characterization and formation kinetics. *Anal Biochem* 2004; **324**: 68–78.
16. Guan F, Villegas G, Teichman J *et al*. Autocrine class 3 semaphorin system regulates slit diaphragm proteins and podocyte survival. *Kidney Int* 2006; **69**: 1564–1569.
17. Harper SJ, Xing CY, Whittle C *et al*. Expression of neuropilin-I by human glomerular epithelial cells *in vitro* and *in vivo*. *Clin Sci* 2001; **101**: 439–446.
18. Wolf G, Haberstroh U, Neilson EG. Angiotensin II stimulates the proliferation and biosynthesis of type I collagen in cultured murine mesangial cells. *Am J Pathol* 1992; **140**: 95–107.
19. Haverty TP, Kelly CJ, Hines WH *et al*. Characterization of a renal tubular epithelial cell line which secretes the autologous target antigen of autoimmune experimental interstitial nephritis. *J Cell Biol* 1988; **107**: 1359–1368.

20. Soker S, Miao HQ, Nomi M *et al*. VEGF165 mediates formation of complexes containing VEGFR-2 and neuropilin-1 that enhance VEGF165-receptor binding. *J Cell Biochem* 2002; **85**: 357–368.

21. Bagri A, Tessier-Lavigne M. Neuropilins as Semaphorin receptors: *in vivo* functions in neuronal cell migration and axon guidance. *Adv Exp Med Biol* 2002; **515**: 13–31.

22. Gallichio MA, McRobert EA, Tikoo A *et al*. Advanced glycation end products inhibit tubulogenesis and migration of kidney epithelial cells in an ezrin-dependent manner. *J Am Soc Nephrol* 2006; **17**: 414–421.

23. Kreuter M, Bielenberg D, Hida Y *et al*. Role of neuropilins and semaphorins in angiogenesis and cancer. *Ann Hematol* 2002; **81**(Suppl 2): S74.

24. Chen G, Sima J, Jin M *et al*. Semaphorin-3A guides radial migration of cortical neurons during development. *Nat Neurosci* 2008; **11**: 36–44.

25. Eremina V, Cui S, Gerber H *et al*. Vascular endothelial growth factor A signaling in the podocyte-endothelial compartment is required for mesangial cell migration and survival. *J Am Soc Nephrol* 2006; **17**: 724–735.

26. Foster RR, Hole R, Anderson K *et al*. Functional evidence that vascular endothelial growth factor may act as an autocrine factor on human podocytes. *Am J Physiol Renal Physiol* 2003; **284**: F1263–F1273.

27. Allombert-Blaise C, Tamiji S, Mortier L *et al*. Terminal differentiation of human epidermal keratinocytes involves mitochondria- and caspase-dependent cell death pathway. *Cell Death Differ* 2003; **10**: 850–852.

28. Ruester C, Bondeva T, Franke S *et al*. Advance glycation endproducts induce cell cycle arrest and hypertrophy in podocytes. *Nephrol Dial Transplant* 2008; **23**: 2179–2191.

29. Cohen MP, Clements RS, Hud E *et al*. Evolution of renal function abnormalities in the db/db mouse that parallels the development of human diabetic nephropathy. *Exp Nephrol* 1996; **4**: 166–171.

30. Cohen CD, Frach K, Schlondorff D *et al*. Quantitative gene expression analysis in renal biopsies: a novel protocol for a high-throughput multicenter application. *Kidney Int* 2002; **61**: 133–140.

31. Gerth J, Cohen CD, Hopfer U *et al*. Collagen type VIII expression in human diabetic nephropathy. *Eur J Clin Invest* 2007; **37**: 767–773.

32. Shankland SJ. The podocyte's response to injury: role in proteinuria and glomerulosclerosis. *Kidney Int* 2006; **69**: 2131–2147.

33. Wolf G, Schroeder R, Thaiss F *et al*. Glomerular expression of p27^{Kip1} in diabetic *db/db* mouse: role of hyperglycemia. *Kidney Int* 1998; **53**: 869–879.

34. Cohen MP, Ziyadeh FN, Hong SW *et al*. Inhibiting albumin glycation *in vivo* ameliorates glomerular overexpression of TGF-β1. *Kidney Int* 2002; **61**: 2025–2032.

35. Yuan L, Moyon D, Pardanaud L *et al*. Abnormal lymphatic vessel development in neuropilin 2 mutants mice. *Development* 2002; **129**: 4797–4806.

36. Villegas G, Tufro A. Ontogeny of semaphorins 3A and 3F and their receptors neuropilins 1 and 2 in the kidney. *Mech Dev* 2002; **119S**: S149–S153.

37. Takashima S, Kitakaze M, Asakura M *et al*. Targeting of both mouse neuropilin-1 and neuropilin-2 genes severely impairs developmental yolk sac and embryonic angiogenesis. *Proc Natl Acad Sci USA* 2002; **99**: 3657–3662.

38. Staton CA, Kumar I, Reed MW *et al*. Neuropilins in physiological and pathological angiogenesis. *J Pathol* 2007; **212**: 237–248.

39. Fuh G, Garcia KC, de Vos AM. The interaction of neuropilin-1 with vascular endothelial growth factor and its receptor flt-1. *J Biol Chem* 2000; **275**: 26690–26695.

40. Soker S, Takashima S, Miao HQ *et al*. Neuropilin-1 is expressed by endothelial and tumor cells as an isoform-specific receptor for vascular endothelial growth factor. *Cell* 1998; **92**: 735–745.

41. Wharram BL, Goyal M, Wiggins JE *et al*. Podocyte depletion causes glomerulosclerosis: diphtheria toxin-induced podocyte depletion in rats expressing human diphtheria toxin receptor transgene. *J Am Soc Nephrol* 2005; **16**: 2941–2952.

42. Guan F, Villegas G, Teichman J *et al*. Autocrine VEGF-A system in podocytes regulates podocin and its interaction with CD2AP. *Am J Physiol Renal Physiol* 2006; **291**: F422–F428.

43. Cohen MP, Lautenslager GT, Hud E *et al*. Inhibiting albumin glycation attenuates dysregulation of VEGFR-1 and collagen IV subchain production and the development of renal insufficiency. *Am J Physiol Renal Physiol* 2007; **292**: F789–F795.

44. Tapia R, Guan F, Gershin I *et al*. Semaphorin 3a disrupts podocyte foot processes causing acute proteinuria. *Kidney Int* 2008; **73**: 733–740.

45. Shankland SJ, Pippin JW, Reiser J *et al*. Podocytes in culture: past, present, and future. *Kidney Int* 2007; **72**: 26–36.

46. Livak KJ, Schmittgen TD. Analysis of relative gene expression data using real-time quantitative PCR and the 2(-Delta Delta C(T)) Method. *Methods* 2001; **25**: 402–408.

47. Panzer U, Thaiss F, Zahner G *et al*. Monocyte chemoattractant protein-1 and osteopontin differentially regulate monocytes recruitment in experimental glomerulonephritis. *Kidney Int* 2001; **59**: 1762–1769.